Journal of Applied Polymer Science

Hydrogel Composites Based on Linear Low-Density Polyethylene-g-Poly (acrylic acid)/Kaolin or Halloysite Nanotubes

Maryam Irani, Hanafi Ismail, Zulkifli Ahmad
School of Materials and Mineral Resources Engineering, USM Engineering Campus, Universiti Sains Malaysia, Nibong Tebal, Penang, Malaysia
Correspondence to: H. Ismail (E-mail: hanafi@eng.usm.my)

ABSTRACT: Two series of superabsorbent hydrogel composites were prepared using waste linear low-density polyethylene, acrylic acid, and two types of clays including kaolin and halloysite nanotube (HNT) through emulsion polymerization. The effects of the clay content on Water absorbency were investigated to obtain a high swelling capacity. The prepared samples were characterized using FTIR, SEM, thermogravimetric analysis, XRD, solid-state ^{13}C Nuclear Magnetic Resonance spectroscopy, and ^{29}Si NMR. SEM characterization of the samples showed that the hydrogel composites have more pores and a higher swelling ratio than the clay-free hydrogels. The hydrogel composite containing kaolin had higher water absorbency compared to the hydrogel composites with HNT. The swelling behavior of the hydrogel composite was investigated in various saline solutions. The hydrogel composite containing 5 wt % kaolin had the highest water absorbency (760 g/g in distilled water). © 2013 Wiley Periodicals, Inc. J. Appl. Polym. Sci. **2014**, *131*, 40101.

KEYWORDS: gels; grafting; clay; composites

Received 2 August 2013; accepted 21 October 2013
DOI: 10.1002/app.40101

INTRODUCTION

Linear low-density polyethylene (LLDPE) is a linear polyethylene (PE) involving alkyl short-chain branches that are incorporated through the insertion of α-olefins (1-butene, 1-octene, etc.) during the polymerization of ethylene.[1] Due to its excellent mechanical properties, LLDPE has been widely used in different applications, such as plastic films.[2] The consumption and waste generation rates of plastic solid waste have been increasing considerably. The disposal of plastics has posed a challenge to waste management, and plastic waste has been regarded as an environmental problem.[3]

There are different alternatives for reducing the problem of their disposal, and for converting them into valuable products, such as polymer modification and functionalization.[4,5] Chemical modification and functionalization of synthetic polymers have been useful methods for increasing their range of applications. For example, graft polymerization of acrylic acid (AA) on waste polymers such as waste polystyrene and polyurethane and converting them into useful products have been recently reported.[6,7]

Hydrogels are defined as hydrophilic three-dimensional polymer networks, with a corresponding absorption capacity of up to 10 g/g.[8] Hydrogels have wide applications in a variety of fields, such as water purification,[8] agriculture,[8–10] drug delivery,[11] tissue engineering,[12] and sensors.[13] Hydrogels are weak and fragile; a common method to reduce this problem is to incorporate clay particles, which can enhance their mechanical properties.[14,15] Different types of clays have been utilized for the preparation of hydrogel composites, such as bentonite,[7] kaolin,[16] montmorillonite,[17] and attapulgite.[18] The type of mineral powder can play an effective role on the absorbent properties of the hydrogel composites.

Kaolin is a 1 : 1 type clay mineral with the chemical formula ($Al_2Si_2O_5(OH)_4 \cdot nH_2O$), composed of silicon tetrahedral sheets and aluminum octahedral sheets, and it is a sheet-like clay.[19] Halloysite nanotube (HNT) is a two-layered aluminosilicate and they are similar to kaolin chemically ($Al_2Si_2O_5(OH)_4 \cdot nH_2O$) but with a hollow nanotubular structure, which is composed of a two-layered alignment of the tetrahedral sheet of silica bonded to the octahedral sheet of alumina.[20] This structure causes the wall to curve into the cylindrical shape.[21] The structures of the kaolin and HNT are shown in Figure 1.

In our previous work,[22] a type of hydrogel composite with waste low-density polyethylene and AA were prepared under optimum conditions and the highest water absorbency for the sample without clay was 600 g/g in distilled water. In this work, superabsorbent hydrogel composites filled with kaolin and HNT were prepared under the same conditions, and the swelling behavior of the samples was investigated.

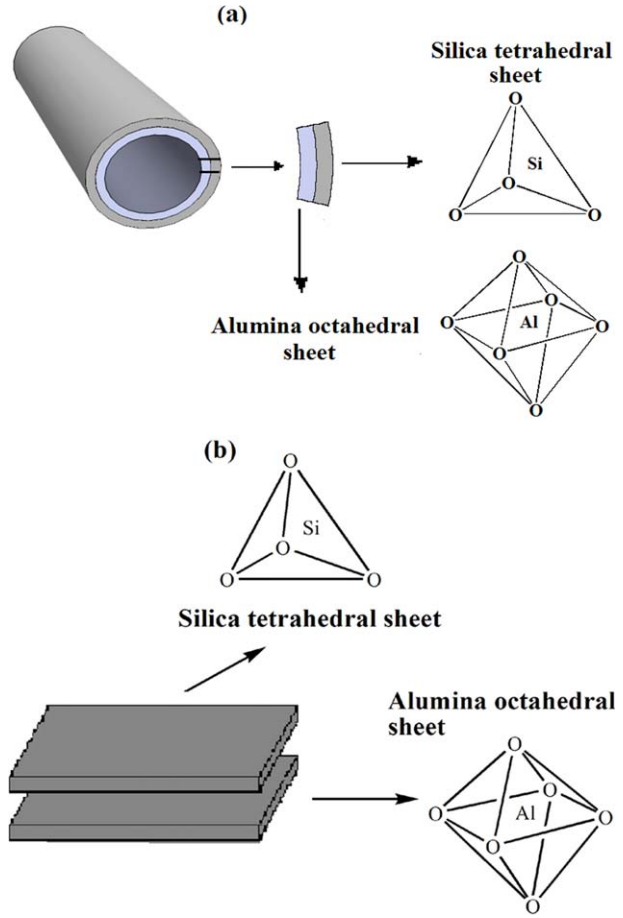

Figure 1. Schematic illustration of (a) HNT and (b) kaolin structures. [Color figure can be viewed in the online issue, which is available at wileyonlinelibrary.com.]

EXPERIMENTAL

Materials

N,*N*′-methylene-bis-acrylamide (MBA, chemically pure, from Aldrich). Benzoyl peroxide (BP) and sodium hydroxide were purchased from Merck. AA (Fluka) was used without purification. Toluene was obtained from Merck, and Sorbitan monostearate (Span 60) was obtained from Aldrich. Waste LLDPE was obtained from Juara One Resources Sdn Bhd, Bukit Mertajam, Penang, Malaysia. The HNT, were supplied by Imerys Tableware Asia Limited, New Zealand. Kaolin was supplied by Ipoh Ceramics Sdn. Bhd, Malaysia.

Instrumental Analysis

FTIR spectra of prepared samples were taken as KBr pellets, using a Perkin-Elmer Spectrum one apparatus. FTIR spectra of the samples were obtained in a range between 4000 and 400 cm^{-1}.

The solid-state CP/MAS NMR experiments were carried out using a Bruker 400 MHz ultrashide spectrometer, operating at 100.577 MHz for ^{13}C and 79.460 MHz for ^{29}Si.

Thermogravimetric analysis (TGA) of the prepared samples was carried out using a Perkin-Elmer Pyris 6 TGA analyzer from 50 to 700°C at a heating rate of 10°C/min, with a nitrogen flow of 10 ml/min.

Micrographs of the prepared samples were collected using a field emission scanning electron microscope (FESEM, ZEISS Supra-35VP). Before the SEM observation, the samples were coated with a thin layer of platinum.

The XRD pattern of clays and hydrogel composites were recorded by a Bruker Axs model D8 diffractometer. The basal spacing of clays and hydrogel composites was calculated using Bragg's law. The Cu Kα ($\lambda = 1.54060$ Å) was operated at 40 kV and 40 mA in combination with a Ni filter, and the scanning range was 5–30°.

A Brookfield viscometer (Brookfield DV- II^+ Viscometer, spindle R4) was used to measure viscosity as a scale of gel strength.[16] 3.0 g of the prepared sample was added to a 600 ml beaker containing 400 ml distilled water. The viscosity was measured after 1 h.

Preparation of Linear Low-Density Polyethylene-g-Poly (acrylic acid) Superabsorbent Hydrogel Composite

Linear low-density polyethylene-*g*-poly (acrylic acid) (LLDPE-*g*-PAA) was synthesized and optimized to get the highest water absorbency (600 g/g), and the procedure for the synthesis of LLDPE-*g*-PAA was discussed earlier in our previous work.[22] Briefly, the preparation of LLDPE-*g*-PAA hydrogel composite consisted of two steps. In the first step, 1 g of waste LLDPE was dissolved in toluene (20 ml) at 90°C in a four-necked reaction flask, equipped with a thermometer, and a mechanical stirrer, under nitrogen flow to remove the oxygen from the system. Then, the temperature was lowered to 60°C, and an appropriate amount of Span 60 (0.3 g) (used as an emulsifier) was added to the solution. After 10 min, a suitable amount of BP (used as an initiator) was added to the solution. In the second step, an exact amount of AA was partially neutralized with sodium hydroxide solution (3 M), cooled (ice bath) and stirred for 5 min, then clay powder, HNT, or kaolin (0.3, 0.5, 0.7, 0.9, and 1.1 g) was dispersed in the above monomer solution when stirred for 15 min. Then the AA solution was added to the reaction flask. After 10 min, an appropriate amount of crosslinker (MBA) was added to the solution. When the solution reached the gel point, the temperature was increased to 70°C for 3 h. Then the samples were washed with ethanol, cut into small pieces, and dried at 80°C for 12 h. This was followed by milling and screening.

Acrylic acid homopolymers and unreacted monomers were extracted from the product by soxhlet extraction, using an ethanol–water mixture (80 : 20) for 24 h.[23] After incorporating the HNT and kaolin clay particles in a polymer matrix, the resulting samples were named LLDPE-*g*-PAA/HNT and LLDPE-*g*-PAA/Kaolin hydrogel composites, respectively.

Property Investigation

Measurements of Equilibrium Water Absorption. A known amount of sample (0.1 ± 0.01 g) with particle sizes between 60 and 100 mesh (150–250 μm) was dispersed in 400 ml of distilled water or 50 ml of saline solution. The samples were then allowed to absorb water at room temperature for 24 h. Then, after the swollen samples were taken out from any excess water

Table I. Effect of Clay Content on the Water Absorbencies of the Superabsorbent Hydrogel Composites

Sample	Clay percentage (wt %)	Q_{H_2O} (g/g)
LLDPE-*g*-PAA	0	600
Hydrogel composites with HNT		
LLDPE-*g*-PAA/HNT_1	3	630
LLDPE-*g*-PAA/HNT_2	5	580
LLDPE-*g*-PAA/HNT_3	7	500
LLDPE-*g*-PAA/HNT_4	9	430
LLDPE-*g*-PAA/HNT_5	11	400
Hydrogel composites with Kaolin		
LLDPE-*g*-PAA/$kaolin_1$	3	650
LLDPE-*g*-PAA/$kaolin_2$	5	760
LLDPE-*g*-PAA/$kaolin_3$	7	580
LLDPE-*g*-PAA/$kaolin_4$	9	490
LLDPE-*g*-PAA/$kaolin_5$	11	430

Reaction conditions: reaction temperature, 70°C; 80% neutralization degree of AA; weight ratio of AA/LLDPE in the feed 9 : 1; weight ratios of oil-soluble initiator, crosslinker, and emulsifier in the feed of 0.35, 0.080, 3.0 wt %.

by filtering via a 100-mesh screen, they were weighed. The swelling absorbency (Q_{H_2O}) of the samples was calculated using the following formula:

$$Q_{H_2O} = (m_2 - m_1)/m_1 \quad (1)$$

where m_2 and m_1 are the weights of swollen gel and the dried gel, respectively.

Swelling Kinetics. The swelling kinetics of hydrogel composites in distilled water was measured according to the following procedure. A series of weighed dried samples (0.05 g) were immersed in distilled water. The swollen samples were separated with a mesh screen and weighed at set intervals (every 15 min). This procedure was repeated until the weight of the swollen samples remained constant. The water absorbency at any given moment was calculated according to eq. (1).

Swelling in Salt Solutions. Water absorbance capacity of the hydrogel composite was investigated in various saline solutions ($FeCl_3$, $CaCl_2$, and NaCl) with different concentrations; according to the method introduced in "Measurements of equilibrium water absorption".

RESULTS AND DISCUSSION

Effect of the Amount of Clay on Water Absorbency

The influence of clay content, HNT, and kaolin, on the water absorbency of the LLDPE-*g*-PAA superabsorbent composite is shown in Table I. It is obvious that the clay content has an important effect on the water absorbency of this superabsorbent composite. According to our previous work,[22] the highest water absorbency without clay was 600 g/g. In the case of LLDPE-*g*-PAA/HNT, the water absorbency of the composite in distilled water increased slightly from 600 to 630 g/g, as 3 wt % of HNT was introduced. In the case of LLDPE-*g*-PAA/kaolin, the water absorbency of the composite increased from 600 to 760 g/g, as 5 wt % of kaolin was introduced in the hydrogel composites. In both cases, according to the FT-IR analysis data from this work ("FTIR spectra analysis"), the —OH groups of clay particles (HNT and Kaolin) could participate in the formation of the composite, which can improve the polymeric network of the hydrogel and increase the water absorbency.

The hydrogel composites showed a decrease in water absorbency with the further incorporation of HNT >3% and kaolin >5% in the hydrogel composites. This could be due to the fact that

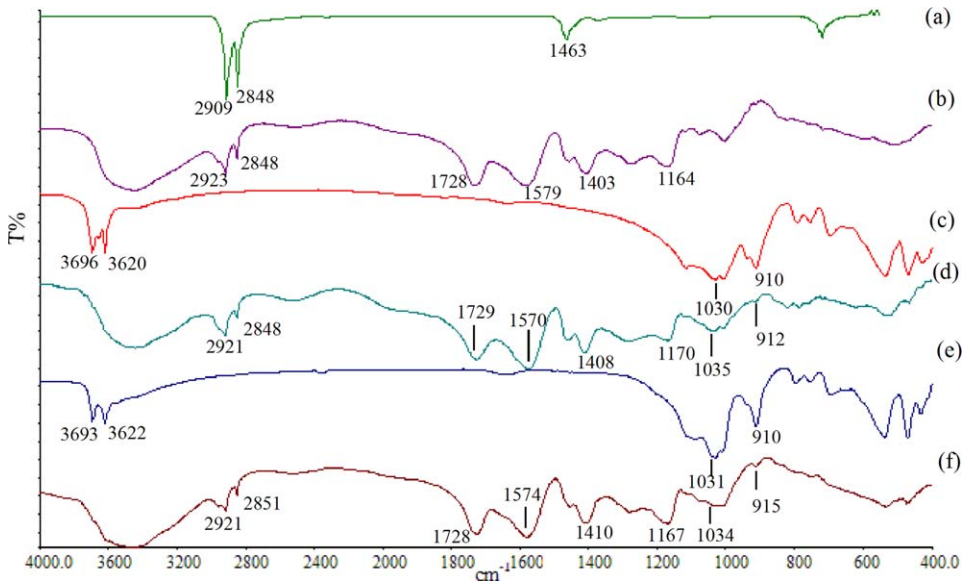

Figure 2. FTIR spectra of (*a*) LLDPE, (*b*) LLDPE-*g*-PAA, (*c*) kaolin, (*d*) LLDPE-*g*-PAA/$kaolin_1$ (composite containing 3 wt % kaolin), (*e*) HNT, and (*f*) LLDPE-*g*-PAA/HNT_1 (composite containing 3 wt % HNT). [Color figure can be viewed in the online issue, which is available at wileyonlinelibrary.com.]

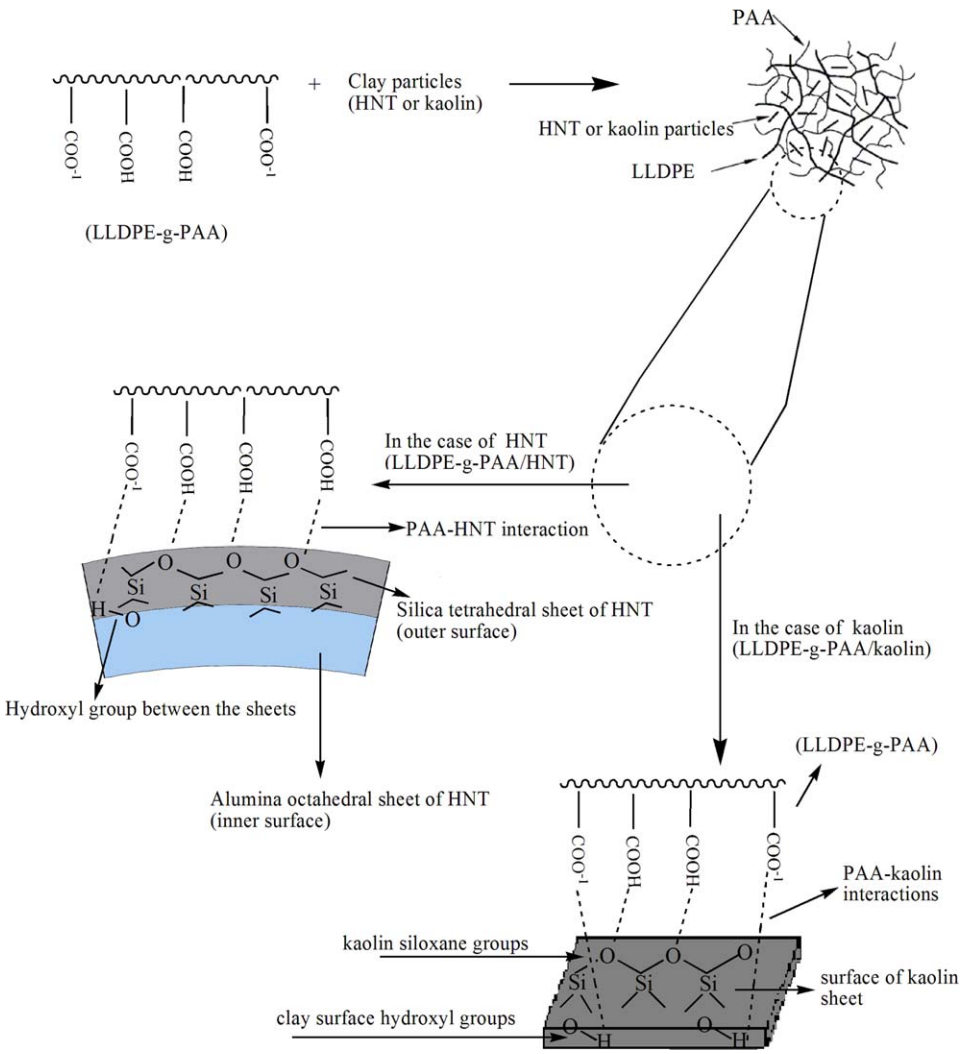

Figure 3. Representative structure of hydrogel composites. [Color figure can be viewed in the online issue, which is available at wileyonlinelibrary.com.]

the interactions between clay particles and AA rose gradually with increasing clay content (HNT or kaolin), which resulted in an increased formation of physical and chemical cross-links in the polymeric network. The elasticity of the polymer chains declined with more cross-linking points in the polymeric network. The water absorbency of the composite declined with decreasing polymer elasticity.[17]

FTIR Spectra Analysis

FTIR spectra of LLDPE, LLDPE-*g*-PAA, HNT, kaolin, and corresponding hydrogel composites incorporated with 3% clays are shown in Figure 2. The FTIR spectrum of LLDPE (Figure 2a) shows two sharp peaks at 2909 and 2843 cm^{-1} that corresponded to the C—H symmetric and asymmetric stretching. Furthermore, CH_2 stretching is also shown at 1463 cm^{-1}. After the grafting of AA (LLDPE-gPAA), new peaks appeared in the spectrum (Figure 2b). These include a C═O stretching band of AA at 1728 cm^{-1}, the symmetric and asymmetric COO^- stretching of AA at 1403 and 1579 cm^{-1}, a C—O band at 1164 cm^{-1} as well as a strong and broad peak at 3450 cm^{-1} that corresponded to the water molecules.

The absorption peaks at 3696, 3620 cm^{-1} in spectra of kaolin, and the absorption peaks at 3693, 3622 cm^{-1} in spectra of HNT contributed to OH group on kaolin and HNT powder, respectively (Figure 2c, e).

After the graft-copolymerization, the —OH stretching of both of the clay (HNT and kaolin) at around 3600 cm^{-1} overlapped with the broad peak of the hydrogen bonding in the region 3400–3700 cm^{-1} (Figure 2d, f). This indicates that the OH groups on kaolin and HNT participated in the reaction. Furthermore, the peak at 1031 cm^{-1} in spectra of HNT and the peak at 1030 cm^{-1} in spectra of kaolin were ascribed to the Si—O bond of HNT and kaolin, respectively. This peak shifted slightly to 1035 and 1034 cm^{-1} in spectra of LLDPE-*g*-PAA/kaolin$_1$ and LLDPE-*g*-PAA/HNT$_1$, respectively.

The peak at 910 cm^{-1} in spectra of HNT and kaolin corresponds to the —OH group in Al_2OH. After copolymerization, this peak shifted slightly to 912 and 915 cm^{-1} in spectra of

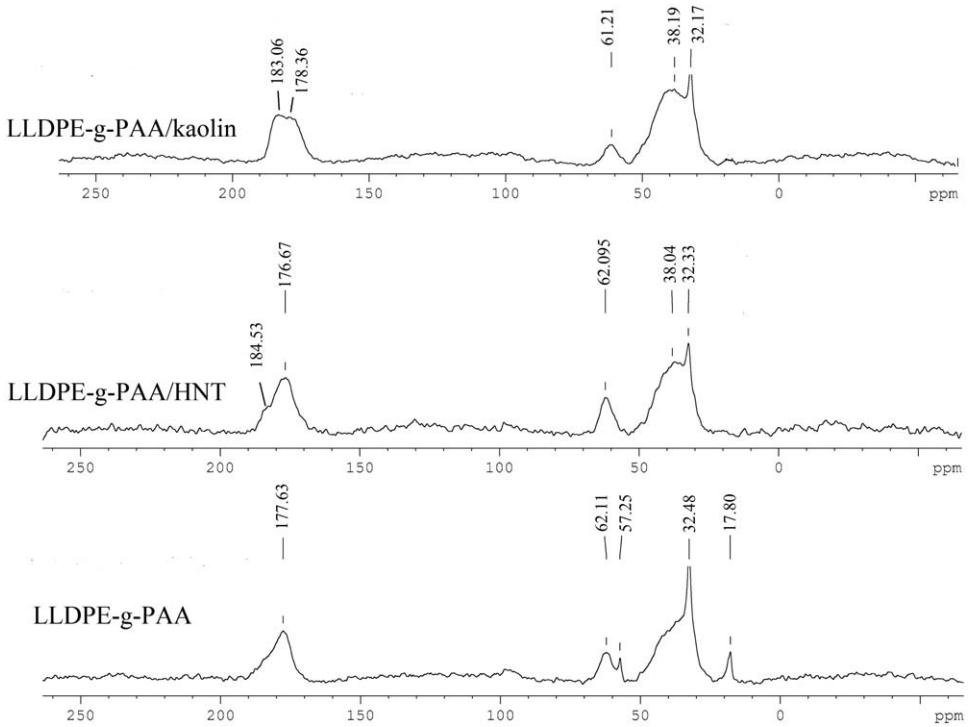

Figure 4. ^{13}C solid-state NMR spectrum of LLDPE-*g*-PAA, LLDPE-*g*-PAA/HNT_1 (composite containing 3 wt % HNT), and LLDPE-*g*-PAA/$kaolin_1$ (composite containing 3 wt % kaolin).

LLDPE-*g*-PAA/$kaolin_1$ and LLDPE-*g*-PAA/HNT_1, respectively. All of these observations show the presence of the clay particles in the formation of the hydrogel composites. A proposed LLDPE-*g*-PAA formation mechanism was illustrated in our previous work.[22] Here, the representative structure of hydrogel composites (interaction between carboxylate groups of polymer matrix and silicate layer of clays) is shown in Figure 3.

^{13}C Nuclear Magnetic Resonance Spectroscopy (^{13}C NMR)

Figure 4 shows the solid-state CP/MAS ^{13}C Nuclear Magnetic Resonance spectroscopy (^{13}C NMR) spectra of LLDPE-*g*-PAA, LLDPE-*g*-PAA/$kaolin_1$, and LLDPE-*g*-PAA/HNT_1.

The spectrum of LLDPE-*g*-PAA showed peaks at 17.80, 32.48, 57.25, 62.11, and 177.63 ppm, which were described in our previous work.[22] Briefly, in the spectrum of LLDPE-*g*-PAA. the broad band at 30–50 ppm is assigned to the CH and CH_2 of PAA, which overlapped with CH, CH_2, and tertiary carbon of LLDPE. Carbonyl carbon of AA was detected at 177.63 ppm. The peak at 62.11 in the LLDPE-*g*-PAA spectrum is related to the C—O of dimer PAA. Residual ethanol during soxhlet extraction was trapped in the sample (LLDPE-*g*-PAA) and the peaks at 57.25 and 17.80 ppm corresponded to the CH_2 and CH_3 of ethanol, respectively. The interesting point is that two peaks at 57.25 and 17.80 ppm in spectra of LLDPE-*g*-PAA, which attributed to the residual ethanol almost disappeared in the spectrum of hydrogel composites (LLDPE-*g*-PAA/$kaolin_1$ and LLDPE-*g*-PAA/HNT_1). This phenomenon can be due to the surface morphology of the hydrogel composites, which showed porosity on the surface (Figure 6). These pores probably helped residual ethanol to exit during the soxhlet extraction compared to the sample without porosity (LLDPE-*g*-PAA).

The main peaks corresponded to LLDPE-*g*-PAA can be observed for LLDPE-*g*-PAA/$kaolin_1$ and LLDPE-*g*-PAA/HNT_1, but there are some differences in chemical shifts of the carbonyl group. The ^{13}C signal of the carbonyl group can be used for the investigation of molecular environment for samples. The peak at 177.68 ppm in spectrum of LLDPE-*g*-PAA corresponded to the carbonyl group. It can be seen that the carbonyl resonance peaks of hydrogel composites (LLDPE-*g*-PAA/$kaolin_1$ and LLDPE-*g*-PAA/HNT_1) were split into two peaks with chemical shifts at 178.36 and 183.08 ppm for LLDPE-*g*-PAA/$kaolin_1$ and with chemical shifts at 176.67 and 184.53 ppm for LLDPE-*g*-PAA/HNT_1. The rising of the new chemical shifts at 183.08 and 184.53 ppm in spectrum of LLDPE-*g*-PAA/$kaolin_1$ and LLDPE-*g*-PAA/HNT_1, respectively, could be due to the formation of hydrogen bonds between carboxyl groups of matrix (LLDPE-*g*-PAA) with the surface of clay. The same results were reported by Chan and Chu[24] that the carbonyl peak of the hybrid materials could be split into two peaks due to the formation of hydrogen bonds from Si—OH group at organic–inorganic interface.

Si-NMR

The solid-state ^{29}Si CP/MAS NMR spectra of HNT, LLDPE-PAA/HNT_1, LLDPE-*g*-PAA/$Kaolin_1$, and Kaolin are shown in Figure 5. ^{29}Si CP/MAS NMR spectra (Figure 5a) depicts Q^3 silicon signal (−91.68 ppm) ascribed to $Si(OSi)_3(OAl)$ groups of halloysite.[25] The slight change (−91.79 ppm) in the ^{29}Si chemicals shift in the spectra of LLDPE-PAA/HNT_1 indicates that the chemical environment of the silicon nuclei of HNT

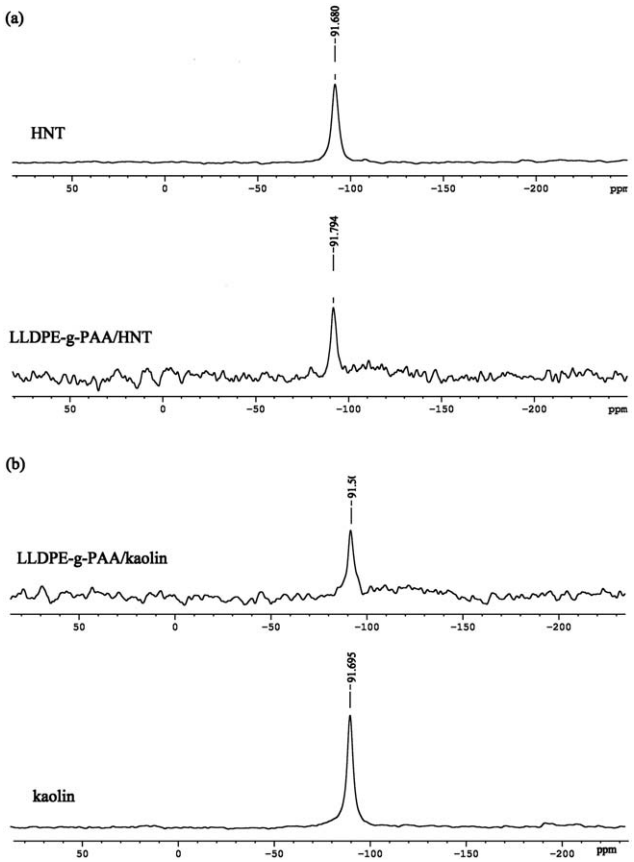

Figure 5. ^{29}Si solid-state NMR spectrum of (a) HNT and LLDPE-*g*-PAA/HNT$_1$ (composite containing 3 wt % HNT) and (b) kaolin, and LLDPE-*g*-PAA/kaolin$_1$ (composite containing 3 wt % kaolin).

incorporation of LLDPE-*g*-PAA changed slightly. Similar results were observed in the LLDPE-*g*-PAA/Kaolin$_1$.

The ^{29}Si MAS NMR spectra of the kaolin and corresponded composite were given in Figure 5b. The ^{29}Si spectrum of kaolin alone is similar to that of HNT. The ^{29}Si MAS NMR spectrum of kaolin shows a single peak at −91.69 ppm corresponding to Q^3 silicon signal structure ($Si(OSi)_3(OAl)$), in agreement with previous literature.[26] The ^{29}Si MAS NMR spectrum of LLDPE-*g*-PAA/Kaolin$_1$ shows a very slight shift to −91.50 ppm. The chemical shift in the spectrum of LLDPE-*g*-PAA/HNT$_1$ and LLDPE-*g*-PAA/kaolin$_1$ compared to the raw clay (HNT and kaolin) shows that there should be an interaction between clay particles and the composite matrix (LLDPE-*g*-PAA), which led to a shifting of the Si peak, and that the chemical environment of Si in the clay platelets changed slightly. From the spectra of FTIR, C-NMR, and Si-NMR, it can be said conclusively that successful incorporation of halloysite (HNT) and kaolin into LDPE-*g*-PAA were achieved.

Morphology Analysis (SEM)

The porosity of a hydrogel can affect its water absorbency.[27] Therefore, the hydrogel microstructure morphology is an important property to investigate. Figure 6 illustrates the SEM micrograph of HNT, kaolin, LLDPE-*g*-PAA, LLDPE-*g*-PAA/HNT, and LLDPE-*g*-PAA/Kaolin. The micrograph of HNT shows that most of the HNTs are tubular in shape, but other morphologies such as pseudo spherical and short tubular can been seen. The raw kaolin shows a flaky and layered structure. SEM image of LLDPE-*g*-PAA shows a smooth surface with few pores. After the incorporation of clay particles (HNT or kaolin) in the polymer matrix, the SEM images show that the hydrogel composites (LLDPE-*g*-PAA/HNT and LLDPE-*g*-PAA/Kaolin) are more porous (higher pore density) than that of LLDPE-*g*-PAA. These pores can be a reason for higher water absorbency of hydrogel composites (LLDPE-*g*-PAA/HNT and LLDPE-*g*-PAA/Kaolin) compared to the hydrogel without clay (LLDPE-*g*-PAA). These pores would provide regions for water penetration into the polymeric network and give more interaction sites for the hydrophilic groups of the polymer network and external stimuli.[17]

X-ray Diffraction

The reaction between clay and LLDPE-*g*-PAA were also investigated by XRD. Figure 7 shows the XRD profile of LLDPE-*g*-PAA, HNT, kaolin, and the corresponded hydrogel composites. The typical diffraction peak and basal spacing from the XRD powder patterns of kaolin, HNT, and the corresponding hydrogel composites incorporated with 3 and 11 percentage clay are presented in Table II.

LLDPE-*g*-PAA shows a peak at $2\theta = 21.32°$, which corresponded to (110) plane of LLDPE, which overlapped with the main peak of PAA. This result was discussed in our previous article.[22]

The HNTs show a diffraction peak at $2\theta = 12.19°$, which corresponded to the 7.25 Å basal spacing for the (001) Plane and another two reflection peaks at (020), (110) bands and (002) plane, which attributed to $2\theta = 20.06°$ and $2\theta = 24.92°$, respectively. According to Figure 7b, a trace of other clay such as sanidine and mica was detected in the samples.[28] Two peaks at $2\theta = 21.89°$ and $2\theta = 26.58°$ are related to mica and sanidine, respectively. The HNTs peaks shifted slightly towards lower angle values in the XRD pattern of LLDPE-*g*-PAA/HNT composites compared to the spacing of the raw HNT (Figure 7b, Table II). However, the increase in the interlayer spacing of the HNT was slightly higher with 3% HNT content (LLDPE-*g*-PAA/HNT$_1$) compared to 11% HNT content in the hydrogel composite (LLDPE-*g*-PAA/HNT$_5$). This result can be due to large amounts of clay that could not be dispersed completely in a polymer matrix and should be in the agglomerated form. Ou[29] found the same result for Poly(trimethylene terephthalate) (PTT)/montmorillonite (MMT) nanocomposites. As there are very slight changes in the basal spacing of HNT in hydrogel composites, there should be limited intercalation of HNT by the polymer matrix. The same results have been reported for ethylene propylene diene monomer/halloysite nanotubes (EPDM/HNT) nanocomposite,[21] and composites based on natural HNTs and natural rubber.[30] From the XRD results, it can be suggested that the polymer matrix should have interacted on the surface of halloysite rather than being incorporated into the lamellae (interlayer) spacing. Therefore, most of the interlayer inner-surface $Al(OH)_3$ groups of HNT could not participate in reaction with the polymer matrix, since they were blocked by the strong hydrogen bonds between layers.[31]

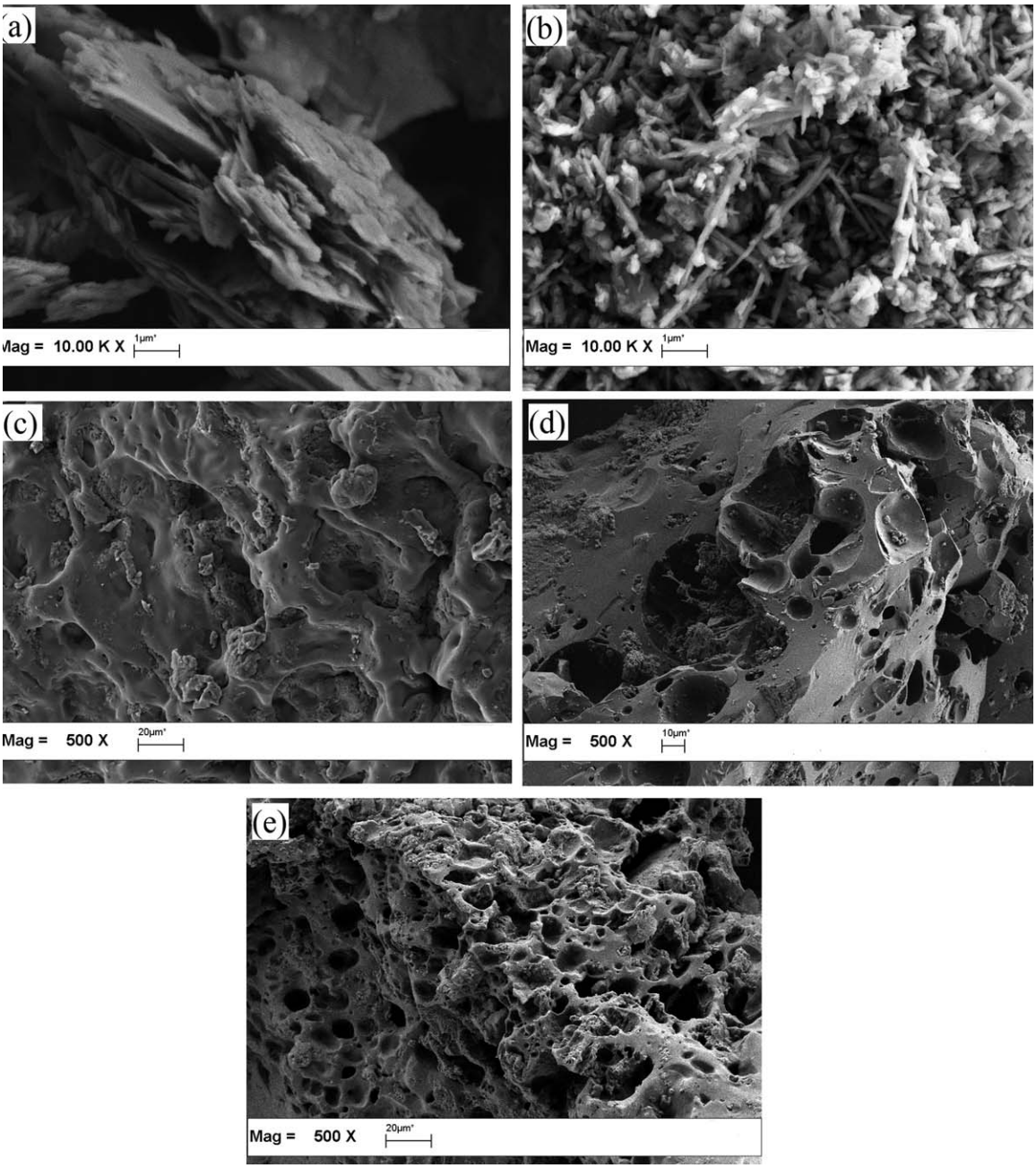

Figure 6. Scanning electron micrographs of (a) kaolin, (b) HNT, (c) LLDPE-*g*-PAA, (d) LLDPE-*g*-PAA/kaolin$_1$ (composite containing 3 wt % kaolin), (e) LLDPE-*g*-PAA/HNT$_1$ (composite containing 3 wt % HNT).

The XRD pattern of kaolin (Figure 7c) contains diffraction peaks at $2\theta = 12.32°$, and $2\theta = 24.84°$, which corresponded to the (001) plane, and (002) plane, respectively. In addition to that, a trace of other minerals such as mica ($2\theta = 8.89°$) and quartz ($2\theta = 19.38°$, $2\theta = 26.63°$) were detected in the kaolin.[32] In the case of LLDPE-*g*-PAA/kaolin composites, the peak corresponded to (001) plane of kaolin shifted slightly toward a higher angle value and the peak corresponded to (002) plane disappeared. It can be suggested that this phenomenon could be due to a slight collapse of the plates that took place during the reaction, which led to the interlayer spacing reduction, at the same time the structure of these hydrogel composites (LLDPE-*g*-PAA/kaolin) appear to be partially exfoliated. The interlayer spacing reduction of clay in polymer composites such as polypropylene/clay composites and chitosan/clay composites have been reported.[33,34]

Thermogravimetric Analysis

Figure 8 depicts the TGA curves of LLDPE-*g*-PAA, LLDPE-*g*-PAA/kaolin$_1$ (composite containing 3 wt % kaolin), LLDPE-*g*-PAA/HNT$_1$ (composite containing 3 wt % HNT), raw HNT, and kaolin. The thermal decomposition temperatures of 10 and 50% weight loss, and char yield of the samples are shown in Table III. It was found that the thermal decomposition

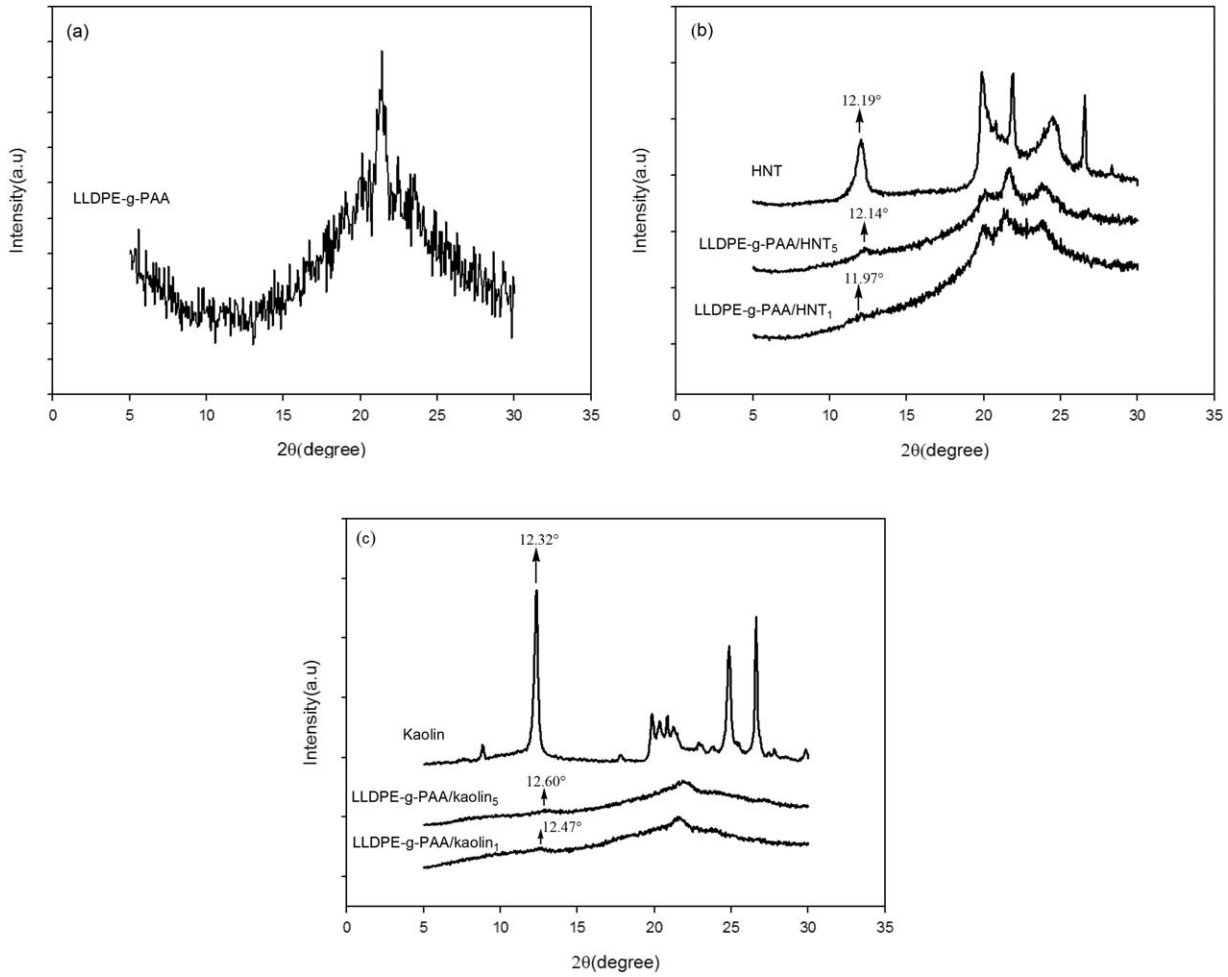

Figure 7. X-ray diffraction patterns of (a) LLDPE-*g*-PAA, (b) HNT, LLDPE-*g*-PAA/HNT_1 (composite containing 3 wt % HNT), LLDPE-*g*-PAA/HNT_5 (composite containing 11 wt % HNT), and (c) kaolin, LLDPE-*g*-PAA/$kaolin_1$ (composite containing 3 wt % kaolin), and LLDPE-*g*-PAA/$kaolin_5$ (composite containing 11 wt % kaolin).

temperature of LLDPE-*g*-PAA was lower compared to that of LLDPE-*g*-PAA/HNT_1 and LLDPE-*g*-PAA/$kaolin_1$. The thermal decomposition temperatures of 10% weight loss for LLDPE-*g*-PAA/$kaolin_1$, LLDPE-*g*-PAA/HNT_1, and LLDPE-*g*-PAA were 215, 181, and 156°C, respectively. The thermal decomposition temperatures of 50% weight loss for LLDPE-*g*-PAA/$kaolin_1$, LLDPE-*g*-PAA/HNT_1, and LLDPE-*g*-PAA were 475, 454, and 342°C, respectively. The char yield for LLDPE-*g*-PAA/$kaolin_1$, LLDPE-*g*-PAA/HNT_1, and LLDPE-*g*-PAA were 31.69, 29.26, and 22.09, respectively. Thermal stability of LLDPE-*g*-PAA/$kaolin_1$ was higher than that of LLDPE-*g*-PAA/HNT_1, which is in agreement with the results for raw HNT and kaolin, which show that thermal stability of raw kaolin was higher than that of HNT. The incorporation of clay particles (HNT or kaolin) into the polymer network leads to an increase in thermal stability compared to the sample without clay (LLDPE-*g*-PAA).

Table II. Diffraction Pattern Characteristics of HNT, Kaolin and Corresponded Hydrogel Composites

Specific plane Diffraction pattern	(001)		(002)		(020),(110)	
	2θ°	d(Å)	2θ°	d(Å)	2θ°	d(Å)
HNT	12.19	7.25	24.92	3.57	20.06	4.42
LLDPE-*g*-PAA/HNT_1	11.97	7.40	23.78	3.73	19.91	4.47
LLDPE-*g*-PAA/HNT_5	12.14	7.33	23.84	3.85	19.98	4.45
Kaolin	12.32	7.19	24.84	3.58	-	-
LLDPE-*g*-PAA/$kaolin_1$	12.47	7.09	-	-	-	-
LLDPE-*g*-PAA/$kaolin_5$	12.60	7.02	-	-	-	-

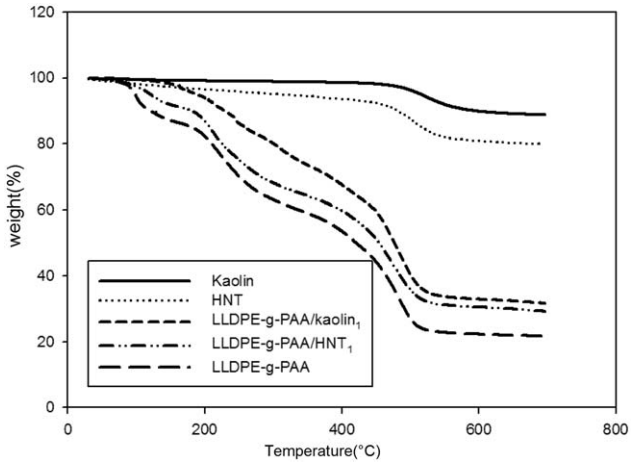

Figure 8. TGA curves of HNT, kaolin, LLDPE-*g*-PAA, and LLDPE-*g*-PAA/kaolin$_1$(composite containing 3 wt % kaolin), and LLDPE-*g*-PAA/HNT$_1$ (composite containing 3 wt % HNT) at a heating rate of 10°C/min.

This phenomenon occurs as a result of the heat barrier effect of clay particles (HNT or kaolin), which enhances the thermal stability of the sample. In addition to that, it can be concluded that the types of clay influences thermal stability of corresponding hydrogel composites. Kaolin could increase the thermal stability of the hydrogel composite to the higher degree compared to when HNT clay is incorporated in the polymer matrix. As the chemical formulas of both types of clay are the same, the structure of these minerals can be a reason for lower thermal stability in HNT than that of kaolin. It is suggested that the heat barrier effects of HNT clay with a tubular structure might be weaker than that of kaolin, which has a layered structure in the prepared hydrogel composites.

Swelling Rates of Composites

The swelling rates of the LLDPE-*g*-PAA and LLDPE-*g*-PAA/HNT$_1$ and LLDPE-*g*-PAA/kaolin$_1$ hydrogel composites are illustrated in Figure 9. It can be seen from Figure 9 that the swelling rates of LLDPE-*g*-PAA, LLDPE-*g*-PAA/HNT, and LLDPE-*g*-PAA/kaolin were higher for 0–45 min and that the water absorbency of LLDPE-*g*-PAA and LLDPE-*g*-PAA/HNT$_1$ and LLDPE-*g*-PAA/kaolin$_1$ reached 260, 330, and 360 g/g within 45 min, respectively. Then the swelling rates of the samples decreased slowly. The results show that LLDPE-*g*-PAA/HNT$_1$ and LLDPE-*g*-PAA/kaolin$_1$ hydrogel composites have similar swelling tendencies and need 145 and 140 min, respectively, to reach water absorbency equilibrium. While the equilibrium of water absorbency for LLDPE-*g*-PAA was reached within 165 min, compared with the swelling rate of LLDPE-*g*-PAA/HNT and LLDPE-*g*-PAA/kaolin, the LLDPE-*g*-PAA superabsorbent took longer to reach equilibrium. The swelling rate of a superabsorbent is determined by surface area, swelling ability, polymer density, and particle size.[35] The results from Figure 9 show that the introduction of clay particles into the polymer network enhanced the swelling rate of the prepared hydrogel. This behavior is probably due to the OH groups located on the surface of clay particles increasing the tendency of the polymeric network to water molecules. Another reason for this behavior may be because hydrogel composites (LLDPE-*g*-PAA/HNT$_1$ and LLDPE-*g*-PAA/kaolin$_1$) have more porosity than the free clay hydrogel (LLDPE-*g*-PAA) (Figure 6), which can provide more free volume for the penetration of water molecules into the polymeric network. As a result, the affinity of the hydrogel network to the water molecules is higher for hydrogel composites than it is for LLDPE-*g*-PAA. Therefore, the time taken to reach equilibrium is lower and the hydrogel composites (LLDPE-*g*-PAA/HNT$_1$ and LLDPE-*g*-PAA/kaolin$_1$) show a faster swelling rate than that of LLDPE-*g*-PAA. The swelling rate of LLDPE-*g*-PAA/HNT$_1$ was slightly lower than that of LLDPE-*g*-PAA/kaolin$_1$, which again can be attributed to the porosity. According to the SEM results, surface of LLDPE-*g*-PAA/kaolin$_1$ seem to have larger pores than that of LLDPE-*g*-PAA/HNT$_1$.

Table III. TGA Data of Prepared Hydrogel Composites and Raw Clays

Sample	$T_{10\%}$	$T_{50\%}$	Char yield
LLDPE-*g*-PAA	156	342	22.09
LLDPE-*g*-PAA/kaolin$_1$	215	475	31.69
LLDPE-*g*-PAA/HNT$_1$	181	454	29.26
Kaolin	592	-	88.73
HNT	481	-	79.88

Gel Strength

The gel strength variation versus rpm of the viscometer spindle for LLDPE-*g*-PAA and LLDPE-*g*-PAA/HNT$_1$, and LLDPE-*g*-PAA/kaolin$_1$ is illustrated in Figure 10. The gel strength of all samples declined with increased rpm of the spindle. The gel strength of LLDPE-*g*-PAA was lower than that of LLDPE-*g*-PAA/HNT$_1$ and LLDPE-*g*-PAA/kaolin$_1$. It can therefore be concluded that clay particles (HNT and kaolin) had an effective role in enhancing gel strength. However, the gel strength of LLDPE-*g*-PAA/kaolin$_1$ was slightly more than that of LLDPE-*g*-PAA/HNT$_1$. This phenomenon is probably due to the difference in their structure, as a tubular structure may lead to weaker gel strength than that of kaolin with a layered structure.

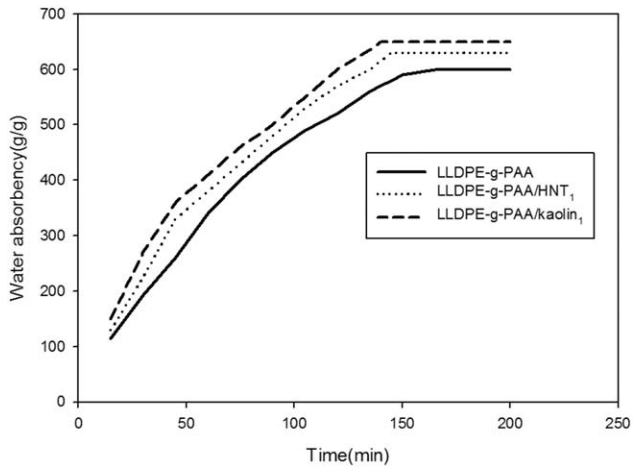

Figure 9. Swelling rate in distilled water for LLDPE-*g*-PAA, LLDPE-*g*-PAA/HNT$_1$ (composite containing 3 wt % HNT) and LLDPE-*g*-PAA/kaolin$_1$ (composite containing 3 wt % kaolin).

Water Absorbency in Various Saline Solutions

Among the prepared samples, the sample containing 5% kaolin (LLDPE-*g*-PAA/kaolin$_2$) had highest water absorbency in distilled water (760 g/g), so this sample was chosen to investigate the effect of saline solutions on water absorbency.

The effect of saline solutions ($FeCl_3$, $CaCl_2$, and NaCl) on water absorbency is shown in Figure 11. The swelling capacity of the hydrogel composite (LLDPE-*g*-PAA/kaolin$_2$) in saline solutions was lower than it was in distilled water. This result could be due to a charge screening effect of the excess cations. These excess cations shield the carboxylate anions and reduce the effective anion–anion repulsion; thus lead to a decrease in the osmotic pressure (ionic pressure) difference between the hydrogel composite network and the external saline solution.[27] Figure 11 shows the swelling capacity of LLDPE-*g*-PAA/kaolin$_2$ in the saline solutions as $Na^+ > Ca^{2+} > Fe^{+3}$. The absorbency of the hydrogel composite in the salt solutions is monovalent > divalent > trivalent cations; the degree of ionic cross-linking rises with increasing cation charge, and consequently, swelling decreases.[36] The decreased water-absorbing capacity observed in multivalent cationic solutions might be attributed to the carboxylate groups, which can induce the formation of the complexes with the cations in saline solutions that create ionic cross-linking points in the polymer network, and resulting in a rise in the network cross-linking density.[37] The ability of the carboxylate group to produce a complex with three cations is $Fe^{3+} > Ca^{2+} > Na^+$, based on their formation constants for ethylenediaminetetraacetic acid (EDTA).[38] In addition to that, water absorbency decreases with increasing concentrations of different external saline solutions. This phenomenon might be due to the presence of cations in the different saline solutions. The osmotic pressure between the external saline solution and the polymeric network decreases with an increasing concentration of the saline solution.[39] The penetration of counter ions (Fe^{+3}, Ca^{2+}, and Na^{+1}) in the polymeric network has a screening effect on the carboxylate groups (—COO—), which causes a declined water absorbency of the hydrogel composites.[27]

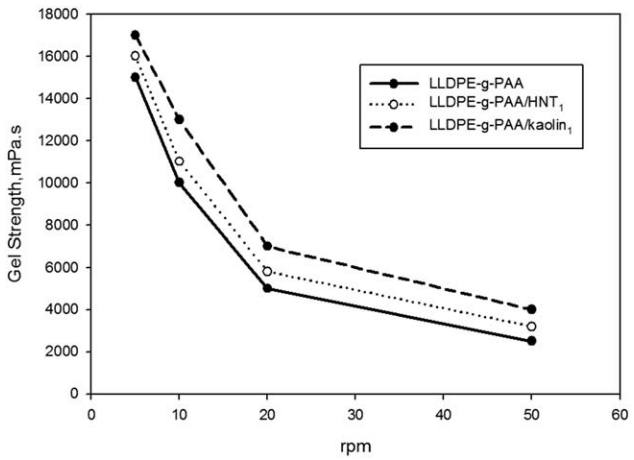

Figure 10. Variation of swollen gel strength with rotation rate of the spindle of a Brookfield viscometer for LLDPE-*g*-PAA, LLDPE-*g*-PAA/HNT$_1$ (composite containing 3 wt % HNT), and LLDPE-*g*-PAA/kaolin$_1$ (composite containing 3 wt % kaolin).

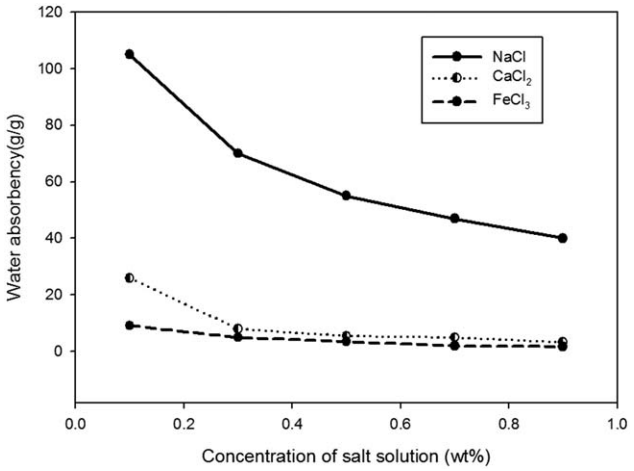

Figure 11. Water absorbency of LLDPE-*g*-PAA/kaolin$_2$ (composite containing 5 wt % kaolin) in NaCl, $CaCl_2$, and $FeCl_3$ in aqueous solutions with various salt concentrations.

CONCLUSIONS

A superabsorbent hydrogel (LLDPE-*g*-PAA) without clay and two series of superabsorbent hydrogel composites (LLDPE-*g*-PAA/HNT and LLDPE-*g*-PAA/kaolin) were synthesized by the graft copolymerization of AA onto waste linear low-density polymer chains (LLDPE) through emulsion polymerization. The incorporation of clay particles resulted in an increase in water absorbency compared to the sample without clay. In comparison between HNT and kaolin on water absorbency, the result showed that the incorporation of kaolin particles in the hydrogel composites resulted in a higher water absorbency compared to the incorporation of HNT particles in the hydrogel composites. FTIR, ^{13}C NMR, and Si NMR results, indicated that there are interactions between the —OH groups of clay particles (HNT and kaolin) and, COOH and —COO^- groups of AA. The XRD analysis showed that the partial exfoliation of kaolin within the hydrogel composites occurs, while a limited intercalation occurs for HNT by the polymer matrix. TGA results show that the introduction of kaolin into the polymeric network resulted in higher thermal decomposition temperatures of the hydrogel composites compared to that of the hydrogel composite with HNT. The gel strength of the samples was also investigated, and it was found that the swollen gel strength of the hydrogel composite with kaolin (LLDPE-*g*-PAA/kaolin) was higher than that of the hydrogel composite with HNT particles (LLDPE-*g*-PAA/HNT). The investigation of LLDPE-*g*-PAA and hydrogel composites swelling rates showed that LLDPE-*g*-PAA/kaolin$_1$ had a higher swelling rate than those of the hydrogel-free clay (LLDPE-*g*-PAA) or hydrogel composite with HNT (LLDPE-*g*-PAA/HNT$_1$). The effect of saline solutions on the water absorbency of LLDPE-*g*-PAA/kaolin$_2$ corresponded to the concentration of saline solution and valence cations. The swelling capacity of the hydrogel composite in the saline solutions (NaCl, $CaCl_2$, and $FeCl_3$) was in the following order: $Na^+ > Ca^{2+} > Fe^{+3}$.

ACKNOWLEDGMENTS

The authors wish to acknowledge the financial support provided by a USM short-term grant (Ac No.: 8044043). Maryam Irani

would like to thank Universiti Sains Malaysia for its financial support under the USM fellowship scheme for her PhD study.

REFERENCES

1. Shin, T. J.; Lee, B.; Seong, B. S.; Han, Y. S.; Lee, C.-H.; Song, H. H.; Stein, R. S.; Ree, M. *Polymer.* **2010**, *51*, 5799.
2. Kontou, E.; Niaounakis, M. *Polymer.* **2006**, *47*, 1267.
3. Nawang, R.; Danjaji, I.; Ishiaku, U.; Ismail, H.; Mohd Ishak, Z. *Polym. Test.* **2001**, *20*, 167.
4. Ramos, V. D.; da Costa, H. M.; Pereira, A. O.; Rocha, M. C. G.; de S.Gomes, A. *Polym. Test.* **2004**, *23*, 949.
5. Subramanian, S.; Lee, S. *J. Appl. Polym. Sci.* **1988**, *70*, 1001.
6. Goel, N. K.; Kumar, V.; Dubey, K. A.; Bhardwaj, Y. K.; Varshney, L. *Radiat. Phys. Chem.* **2013**, *82*, 85.
7. Ismail, H.; Irani, M.; Ahmad, Z. *J. Appl. Polym. Sci.* **2013**, *127*, 4195.
8. Ismail, H.; Irani, M.; Ahmad, Z. *Int. J. Polym. Mater.* **2012**, *62*, 411.
9. Guo, M.; Liu, M.; Zhan, F.; Wu, L. *Ind. Eng. Chem. Res.* **2005**, *44*, 4206.
10. Karadağ, E.; Üzüm, Ö. B.; Saraydın, D.; Güven, O. *Mater. Des.* **2006**, *27*, 576.
11. Wu, D.-Q.; Wang, T.; Lu, B.; Xu, X.-D.; Cheng, S.-X.; Jiang, X.-J.; Zhang, X.-Z.; Zhuo, R.-X. *Langmuir.* **2008**, *24*, 10306.
12. Khan, F.; Tare, R. S.; Oreffo, R. O.; Bradley, M. *Angew. Chem.* **2009**, *121*, 996.
13. Lee, Y. J.; Braun, P. V. *Adv. Mater.* **2003**, *15*, 563.
14. Tongwa, P.; Nygaard, R.; Bai, B. *J. Appl. Polym. Sci.* **2013**, *128*, 787.
15. Haraguchi, K.; Takehisa, T.; Fan, S., *Macromolecules.* **2002**, *35*, 10162.
16. Kabiri, K.; Zohuriaan-Mehr, M. *Polym. Adv. Technol.* **2003**, *14*, 438.
17. Zhang, J.; Wang, L.; Wang, A. *Ind. Eng. Chem. Res.* **2007**, *46*, 2497.
18. Li, A.; Zhang, J.; Wang, A. *Bioresour. Technol.* **2007**, *98*, 327.
19. Cheng, H.; Liu, Q.; Yang, J.; Ma, S.; Frost, R. L. *Thermochim. Acta.* **2012**, *545*, 1.
20. Chao, C.; Zhang, B.; Zhai, R.; Xiang, X.; Liu, J.; Chen, R. *ACS Sustain. Chem. Eng.* **2013**, dx.doi.org/10.1021/sc400199v.
21. Ismail, H.; Pasbakhsh, P.; Fauzi, M. N. A.; Abu Bakar, A. *Polym. Test.* **2008**, *27*, 841.
22. Irani, M.; Ismail, H.; Ahmad, Z. *Polym. Test.* **2013**, *32*, 502.
23. Teli, M.; Waghmare, N. G. *Carbohydr. Polym.* **2009**, *78*, 492.
24. Chan, C.-K.; Chu, I. *Polymer.* **2001**, *42*, 6823.
25. Zhang, Y.; Fu, L.; Yang, H. *Colloid. Surf. A.* **2012**, *44*, 115.
26. Du, C.; Yang, H. *J. Colloid. Interf. Sci.* **2012**, *369*, 216.
27. Bao, Y.; Ma, J.; Li, N., *Carbohydr. Polym.* **2011**, *84*, 76.
28. Hashemifard, S.; Ismail, A.; Matsuura, T. *J. Colloid. Interf. Sci.* **2011**, 359, 359.
29. Ou, C. F., *J. Polym. Sci. Part B. Polym. Phys.* **2003**, *41*, 2902.
30. Rooj, S.; Das, A.; Thakur, V.; Mahaling, R. N.; Bhowmick, A. K.; Heinrich, G. *Mater. Des.* **2010**, *31*, 2151.
31. Yuan, P.; Southon, P. D.; Liu, Z.; Green, M. E. R.; Hook, J. M.; Antill, S. J.; Kepert, C. J. *J. Phys. Chem. C.* **2008**, *112*, 15742.
32. Rakić, V.; Rajić, N.; Daković, A.; Auroux, A. *Microporous. Mesoporous. Mater.* **2013**, *166*, 185.
33. Rohlmann, C. O.; Horst, M. F.; Quinzani, L. M.; Failla, M. D. *Eur. Polym. J.* **2008**, *44*, 2749.
34. Zhao, X.; Mai, Z.; Kang, X.; Dai, Z.; Zou, X. *Electrochim. Acta.* **2008**, *53*, 4732.
35. Zhang, J.; Li, A.; Wang, A. *Carbohydr. Polym.* **2006**, *65*, 150.
36. Pourjavadi, A.; Barzegar, S.; Zeidabadi, F. *React. Funct. Polym.* **2007**, *67*, 644.
37. Castel, D.; Ricard, A.; Audebert, R. *J. Appl. Polym. Sci.* **1990**, *39*, 11.
38. Zhang, J. P.; Li, A.; Wang, A. Q. *Polym. Adv. Technol.* **2005**, *16*, 813.
39. Murali Mohan, Y.; Keshava Murthy, P.; Mohana Raju, K. *React. Funct. Polym.* **2005**, *63*, 11.